Journal of Sound and Vibration (1999) **225**(4), 723–740
Article No. jsvi.1999.2261, available online at http://www.idealibrary.com on IDEAL®

MAXIMIZATION OF THE FUNDAMENTAL FREQUENCIES OF LAMINATED CYLINDRICAL SHELLS WITH RESPECT TO FIBER ORIENTATIONS

H.-T. HU AND J.-Y. TSAI

Department of Civil Engineering, National Cheng Kung University, Tainan, Taiwan 701, *R.O.C.*

(*Received* 6 *August* 1998, *and in final form* 10 *March* 1999)

The fundamental frequencies of fiber-reinforced laminated cylindrical shells with a given material system are maximized with respect to fiber orientations by using the golden section method. The significant effects of shell thickness, shell length, cutout and end condition on the maximum fundamental frequencies and the associated optimal fiber orientations are demonstrated.

© 1999 Academic Press

1. INTRODUCTION

Due to light weight and high strength, the use of fiber-composite laminated materials in aerospace and hydrospace applications have increased rapidly in recent years. The cylindrical shell configuration is widely used in aircraft fuselages, launch-vehicle structures, spacecraft, satellites and pressure hulls of submersibles, which are frequently subjected to dynamic loads in service. Hence, a knowledge of dynamic characteristics of cylindrical shells constructed of fiber-reinforced laminated materials, such as their fundamental frequencies, is essential [1–4].

The fundamental frequencies of fiber-reinforced laminated cylindrical shells depend highly on ply orientations, end conditions, and geometric variables such as thickness, shell length and cutout [4–12]. Therefore, for composite laminated cylindrical shells with a given material system, geometric shape, thickness and end condition, the proper selection of appropriate lamination to maximize the fundamental frequency of the shells becomes an interesting problem [13–15]. However, in spite of the high potential for improved dynamic performance by use of composite optimization, there has not been much of an activity in this area [16].

Research on the subject of structural optimization has been reported by many investigators [17]. Among various optimization schemes, the golden section method is a popular technique and is easily programmed for solution on the computer [18, 19]. In this investigation, optimization of fiber-reinforced laminated cylindrical shells to maximize their fundamental frequencies with respect to fiber

0022-460X/99/340723 + 18 $30.00/0 © 1999 Academic Press

orientations is performed by using the golden section method. The fundamental frequencies of laminated cylindrical shells are calculated by using the ABAQUS finite element program [20]. In the paper, the constitutive equations for fiber-composite lamina and golden section method are briefly reviewed. Then the effects of end condition, thickness, shell length, and cutout on the maximum fundamental frequencies and the associated optimal fiber orientations of composite laminated cylindrical shells is presented. Finally, important conclusions are drawn from the study.

2. CONSTITUTIVE MATRIX FOR FIBER-COMPOSITE LAMINAE

In the finite element analysis, the laminated cylindrical shells are modelled by eight-node isoparametric shell elements with six degrees of freedom per node (three displacements and three rotations). The doubly curved shell element has four edges (three nodes per edge) and can be used to model fairly complicated curved surface structures very accurately. The reduced integration rule together with hourglass stiffness control is employed to formulate the element stiffness matrix [20]. During the analysis, the constitutive matrices of composite materials at element integration points must be calculated before the stiffness matrices are assembled from element level to global level. For fiber-composite laminated materials, each lamina can be considered as an orthotropic layer in a plane stress condition (Figure 1). The stress–strain relations for a lamina in the material co-ordinates (1,2,3) at an element integration point can be written as

$$\{\sigma'\} = [Q_1']\{\varepsilon'\}, \qquad \{\tau'\} = [Q_2']\{\gamma'\}, \tag{1}$$

$$[Q_1'] = \begin{bmatrix} \dfrac{E_{11}}{1-\nu_{12}\nu_{21}} & \dfrac{\nu_{12}E_{22}}{1-\nu_{12}\nu_{21}} & 0 \\ \dfrac{\nu_{21}E_{11}}{1-\nu_{12}\nu_{21}} & \dfrac{E_{22}}{1-\nu_{12}\nu_{21}} & 0 \\ 0 & 0 & G_{12} \end{bmatrix}, \qquad [Q_2'] = \begin{bmatrix} \alpha_1 G_{13} & 0 \\ 0 & \alpha_2 G_{23} \end{bmatrix}, \tag{2}$$

where $\{\sigma'\} = \{\sigma_1, \sigma_2, \tau_{12}\}^{\mathrm{T}}$, $\{\tau'\} = \{\tau_{13}, \tau_{23}\}^{\mathrm{T}}$, $\{\varepsilon'\} = \{\varepsilon_1, \varepsilon_2, \gamma_{12}\}^{\mathrm{T}}$, $\{\gamma'\} = \{\gamma_{13}, \gamma_{23}\}^{\mathrm{T}}$. The α_1 and α_2 are shear correction factors, which are calculated in ABAQUS by assuming that the transverse shear energy through the thickness of laminate is equal to that in unidirectional bending [20, 21]. The constitutive equations for the lamina in the element co-ordinates (x, y, z) become

$$\{\sigma\} = [Q_1]\{\varepsilon\}, \qquad [Q_1] = [T_1]^T[Q_1'][T_1], \tag{3}$$

$$\{\tau\} = [Q_2]\{\gamma\}, \qquad [Q_2] = [T_2]^T[Q_2'][T_2], \tag{4}$$

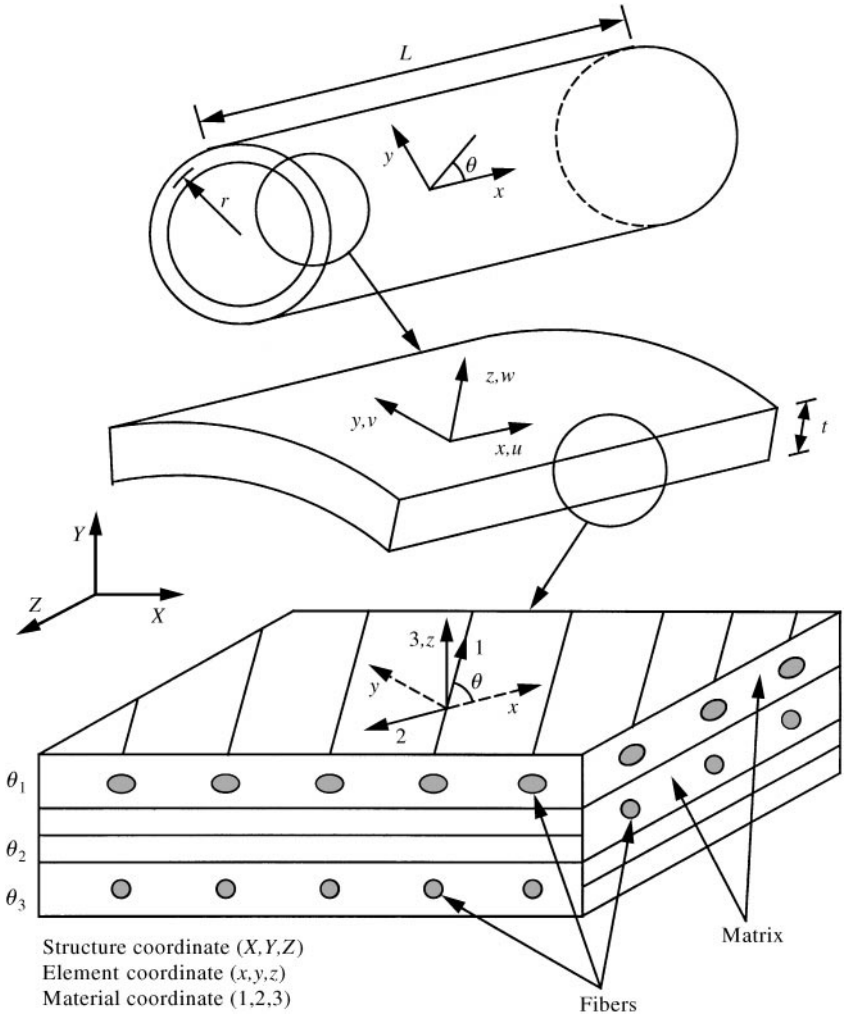

Figure 1. Material, element and structure co-ordinates of fiber-composite laminated cylindrical shell.

$$[T_1] = \begin{bmatrix} \cos^2\theta & \sin^2\theta & \sin\theta\cos\theta \\ \sin^2\theta & \cos^2\theta & -\sin\theta\cos\theta \\ -2\sin\theta\cos\theta & 2\sin\theta\cos\theta & \cos^2\theta - \sin^2\theta \end{bmatrix}$$

$$[T_2] = \begin{bmatrix} \cos\theta & \sin\theta \\ -\sin\theta & \cos\theta \end{bmatrix}, \tag{5}$$

where $\{\sigma\} = \{\sigma_x, \sigma_y, \tau_{xy}\}^T$, $\{\tau\} = \{\tau_{xz}, \tau_{yz}\}^T$, $\{\varepsilon\} = \{\varepsilon_x, \varepsilon_y, \gamma_{xy}\}^T$, $\{\gamma\} = \{\gamma_{xz}, \gamma_{yz}\}^T$, and θ is measured counterclockwise about the z-axis from the element local x-axis to the material 1-axis. The element co-ordinate system (x, y, z) is a curvilinear local system (Figure 1) that is different from the structural global co-ordinate (X, Y, Z).

While the element x-axis is parallel to the longitudinal direction of the cylindrical shell, the element y- and z-axis are in the circumferential and the radial directions of the cylindrical shell. Let $\{\varepsilon_o\} = \{\varepsilon_{xo}, \varepsilon_{yo}, \gamma_{xyo}\}^T$ be the in-plane strains at the mid-surface of the laminate section $\{\kappa\} = \{\kappa_x, \kappa_y, \kappa_{xy}\}^T$ the curvatures, and h the total thickness of the section. If there are n layers in the layup, the stress resultants, $\{N\} = \{N_x, N_y, N_{xy}\}^T$, $\{M\} = \{M_x, M_y, M_{xy}\}^T$ and $\{V\} = \{V_x, V_y\}^T$, can be defined as

$$\begin{Bmatrix} \{N\} \\ \{M\} \\ \{V\} \end{Bmatrix} = \int_{-h/2}^{h/2} \begin{Bmatrix} \{\sigma\} \\ z\{\sigma\} \\ \{\tau\} \end{Bmatrix} \mathrm{d}z$$

$$= \sum_{j=1}^{n} \begin{bmatrix} (z_{jt} - z_{jb})[Q_1] & \frac{1}{2}(z_{jt}^2 - z_{jb}^2)[Q_1] & [0] \\ \frac{1}{2}(z_{jt}^2 - z_{jb}^2)[Q_1] & \frac{1}{3}(z_{jt}^3 - z_{jb}^3)[Q_1] & [0] \\ [0]^T & [0]^T & (z_{jt} - z_{jb})[Q_2] \end{bmatrix} \begin{Bmatrix} \{\varepsilon_o\} \\ \{\kappa\} \\ \{\gamma\} \end{Bmatrix}, \tag{6}$$

where z_{jt} and z_{jb} are the distances from the mid-surface of the section to the top and the bottom of the jth layer respectively. The [0] is a 3×2 matrix with all the coefficients equal to zero.

3. GOLDEN SECTION METHOD

The golden section method is a popular technique to estimate the maximum, minimum, or zero of a one-variable function [18, 19]. We begin by presenting the method for determining the minimum of the unimodal function F, which is a function of the independent variable X. It is assumed that the lower bound X_L and the upper bound X_U on X are known and that they bracket the minimum (Figure 2). In addition, we assume that the function has been evaluated at both bounds and the corresponding values are F_L and F_U. Now, we can pick up two intermediate points X_1 and X_2 such that $X_1 < X_2$, and evaluate the function at these two points to provide F_1 and F_2. Since F_1 is greater than F_2, now X_1 forms a new lower bound and we have a new set of bounds, X_1 and X_U. We can now select an additional point, X_3, for which we evaluate F_3. It is clear that F_3 is greater than F_2, so X_3 replaces X_U as the new upper bound. Repeating this process, we can narrow the bounds to whatever tolerance is desired.

To determine the method for choosing the interior points $X_1, X_2, X_3, \ldots$, we pick the values of X_1 and X_2 to be symmetric about the center of the interval so that

$$X_U - X_2 = X_1 - X_L \tag{7}$$

In addition, the values of X_1 and X_2 must satisfy the following relationship:

$$\frac{X_1 - X_L}{X_U - X_L} = \frac{X_2 - X_1}{X_U - X_1}. \tag{8}$$

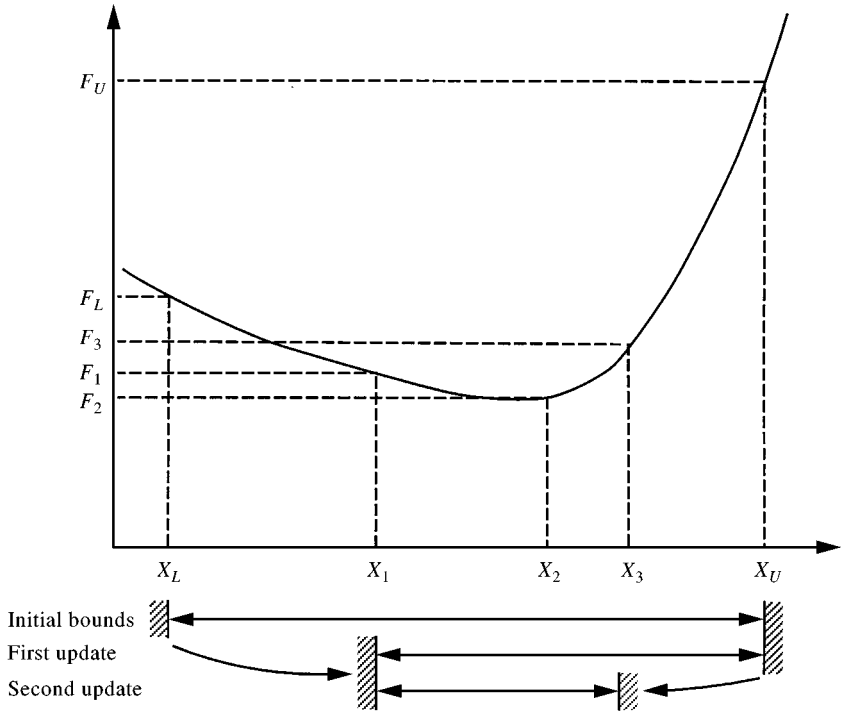

Figure 2. The golden section method.

Let τ be a number between 0 and 1. We can define the interior point X_1 and X_2 to be

$$X_1 = (1 - \tau) X_L + \tau X_U, \qquad X_2 = \tau X_L + (1 - \tau) X_U. \tag{9a, b}$$

Substituting Equations (9a) and (9b) into Equation (8), we obtain

$$\tau^2 - 3\tau + 1 = 0. \tag{10}$$

The above equation has two roots which are 0·38197 and 2·61803. We can ignore the second root since it is greater than 1. Hence, $\tau = 0{\cdot}38197$. The ratio $(1 - \tau)/\tau = 1{\cdot}61803$ is the famous "golden section" number. A detailed "flow diagram" of the golden section algorithm can be obtained in reference [18], and is not duplicated here. For a problem involving the estimation of the maximum of a one-variable function F, we need only minimize the negative of the function, i.e. minimize $-F$.

4. CONVERGENCE STUDY

Prior to the numerical analysis, a convergence study of the eight-node shell element has been performed to analyze an isotropic square plate with four simply supported edges. The thickness of the plate is 0·001 m and the length of one side of the plate is 0·1 m. The material properties are: $E = 206$ GPa, $v = 0{\cdot}3$, and

$\rho = 20{\cdot}29$ kg/m^3. The analytical solution for the fundamental frequency of the plate is $\omega = 60188$ s^{-1}. In the numerical analysis, it is found that the use of 4×4 mesh (16 shell elements) to model the plate gives the same fundamental frequency as the exact solution. On the basis of this result and previous experience on the analyses of composite shells [15], it was decided to use at least 96 elements (32 rows in circumferential direction and 3 rows in longitudinal direction) to model the laminated cylindrical shells having L/r ratio equal to 1. For cylindrical shells with large L/r ratios or with cutouts, more elements are employed to model the entire structures.

5. NUMERICAL ANALYSIS

5.1. LAMINATED CYLINDRICAL SHELLS WITH VARIOUS LENGTHS AND END CONDITIONS

In this section composite laminated cylindrical shells with three types of end conditions (Figure 3(a)) are considered, which are two ends fixed (denoted by FF), one end simply supported and the other end fixed (denoted by SF), and the two ends simply supported (denoted by SS). The radius of the shell, r, is equal to 10 cm and the length of the shell, L, varies from 10 cm to 40 cm. The laminate layups of the shells are $[\pm\theta/90_2/0]_{ns}$ and the thickness of each ply is 0·125 mm. In order to study the effects of shell thickness on the results of optimization, $n = 2$ (20-ply thin

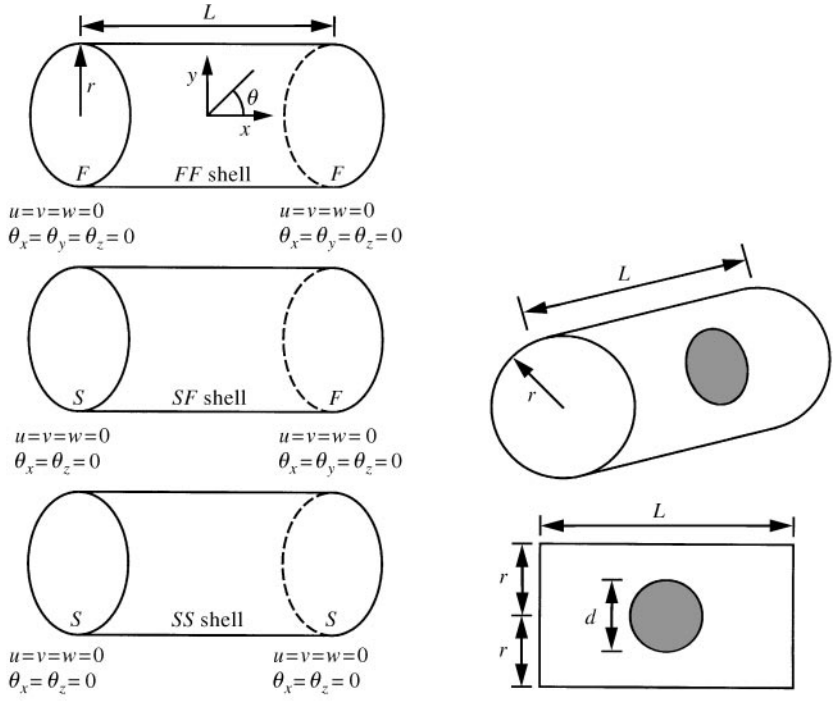

(a) Shells with various end conditions (b) Shells with central circular cutout

Figure 3. Laminated cylindrical shells.

shell) and 10 (100-ply thick shell) are selected for analysis. The reason for using the $[\pm\theta/90_2/0]_{ns}$ layup is typically for the submersible structure applications. When a cylindrical shell is subjected to hydrostatic compression, the stress in the hoop direction is twice that in the longitudinal direction. The selected laminate layup thus renders the stresses of the fibers in both directions at about the same level. The fibers in the $\pm\theta$ directions are primarily used to resist the shear stress. The lamina consists of Graphite/Epoxy and material constitutive properties are taken from Crawley [22], which are $E_{11} = 128$ GPa, $E_{22} = 11$ GPa, $\nu_{12} = 0{\cdot}25$, $G_{12} = G_{13} = 4{\cdot}48$ GPa, $G_{23} = 1{\cdot}53$ GPa, $\rho = 1{\cdot}5 \times 10^3$ kg/m^3. In the analysis, no symmetry simplifications are made for those shells.

For free vibration finite element analysis of composite cylindrical shells, we can obtain the eigenvalue expression as [23]

$$([K] - \omega^2[M])\{D\} = \{0\}. \tag{11}$$

The $[K]$ is a structural stiffness matrix, $[M]$ a structural mass matrix, ω the frequency (eigenvalue), and $\{D\}$ an eigenvector containing the free vibration mode. In ABAQUS, a subspace iteration procedure [20, 24] is used to solve the natural frequency and the eigenvectors. The smallest natural frequency (fundamental frequency) obtained is then the objective function for maximization.

Based on the golden section method, the optimization problem becomes:

$$\text{Maximize: } \omega(\theta) \tag{12a}$$

$$\text{Subjected to: } 0^\circ \leqslant \theta \leqslant 90^\circ. \tag{12b}$$

Before the golden section method is carried out, the fundamental frequency ω of the laminated cylindrical shell is calculated by employing the ABAQUS finite element program for every 10° increment in the θ angle to locate the maximum point approximately. Then proper upper and lower bounds are selected and the golden section method is performed. The optimization process is terminated when an absolute tolerance (the difference of the two intermediate points between the upper bound and the lower bound) $\Delta\theta \leqslant 0{\cdot}5^\circ$ is reached.

Figure 4 shows the optimal fiber angle θ and the associated optimal fundamental frequency ω with respect to the L/r ratio for thin ($[\pm\theta/90_2/0]_{2s}$) laminated cylindrical shells. From Figure 4(a) we can see that the optimal fiber angle θ of the cylindrical shells usually varies between 40° and 50°. The only exception is that when the L/r ratio is close to 2·5, the optimal fiber angle may approach 57°. It seems that the optimal solution may correspond to one mode with L/r below 2·5 and a different mode with L/r above 2·5. Generally, under the same L/r ratio, the shell with two simply supported ends has the largest value for the optimal fiber angle. In addition, the optimal fiber angle seems to be more sensitive to the end conditions when $L/r < 2{\cdot}5$ and less sensitive to the end conditions when $L/r > 2{\cdot}5$. Figure 4(b) shows that under the same L/r ratio, the optimal fundamental frequency is highest for a shell with two fixed ends and lowest for a shell with two simply supported ends. The optimal fundamental frequencies of these shells decrease with increasing shell length. However, the optimal fundamental frequencies seem to be less sensitive to the end conditions when the L/r ratio becomes large.

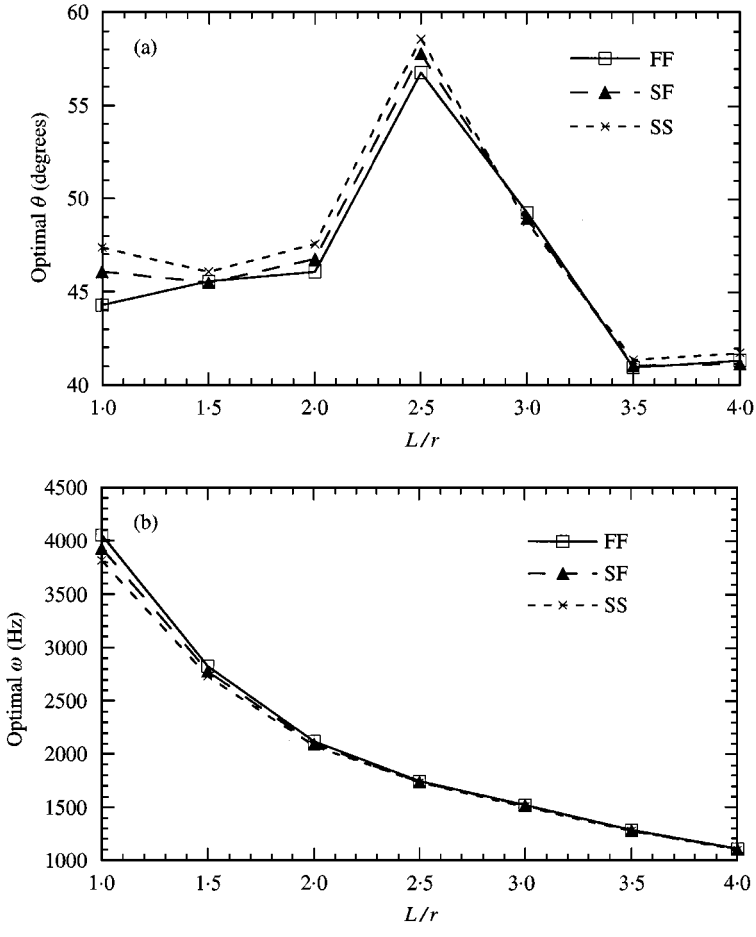

Figure 4. Effects of end conditions and L/r ratio on optimal fiber angle and optimal fundamental frequency of thin ($[\pm\theta/90_2/0]_{2s}$) laminated cylindrical shells ($r = 10$ cm). (a) Optimal fiber angle θ versus L/r ratio; (b) Optimal fundamental frequency ω versus L/r ratio.

Figure 5 shows the optimal fiber angle θ and the associated optimal fundamental frequency ω with respect to the L/r ratio for thick ($[\pm\theta/90_2/0]_{10s}$) laminated cylindrical shells. From Figure 5(a) we can see that the optimal fiber angle θ of the cylindrical shells usually varies between 42° and 46°. When L/r ratio is large (say $L/r > 2{\cdot}5$), the optimal fiber angles of these shells seem to approach constant values. Again, under the same L/r ratio, the shell with two simply supported ends usually has the largest value for the optimal fiber angle. Comparing Figure 5(a) with Figure 4(a), we can observe that the range of the optimal fiber angle for thick laminated cylindrical shells is narrower than that for thin shells. Figure 5(b) shows the similar trend as Figure 4(b). However, under the same L/r ratio, the fundamental frequency of the thick shell is much higher than that of the thin shell.

Figure 6 shows the typical fundamental vibration modes for both thin and thick ($[\pm\theta/90_2/0]_{2s}$ and $[\pm\theta/90_2/0]_{10s}$) shells with two fixed ends and under the

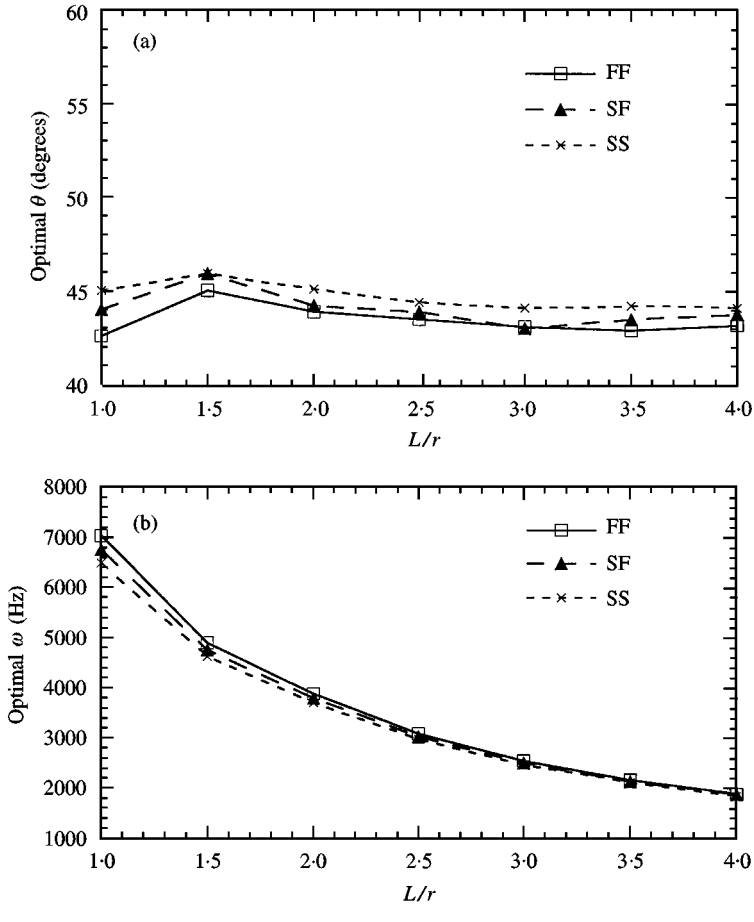

Figure 5. Effects of end conditions and L/r ratio on optimal fiber angle and optimal fundamental frequency of thick ($[\pm\theta/90_2/0]_{10s}$) laminated cylindrical shells ($r = 10$ cm). (a) Optimal fiber angle θ versus L/r ratio; (b) Optimal fundamental frequency ω versus L/r ratio.

optimal fiber orientation. We can find that when the shell length or the shell thickness increases, the vibration modes of these cylindrical shells have fewer waves in the circumferential direction. Similar results are also obtained for shells with other end conditions [25].

5.2. LAMINATED CYLINDRICAL SHELLS WITH VARIOUS CENTRAL CIRCULAR CUTOUTS AND END CONDITIONS

In this section, laminated cylindrical shells with $r = 10$ cm and $L = 20$ cm are analyzed. These shells contain central circular cutouts with diameter d varying between 0 cm and 12 cm (Figure 3(b)). As before, three types of end conditions and two laminate layups, $[\pm\theta/90_2/0]_{2s}$ and $[\pm\theta/90_2/0]_{10s}$, are selected for analysis.

Figure 7 shows the optimal fiber angle θ and the associated optimal fundamental frequency ω with respect to the ratio d/r for thin ($[\pm\theta/90_2/0]_{2s}$) laminated

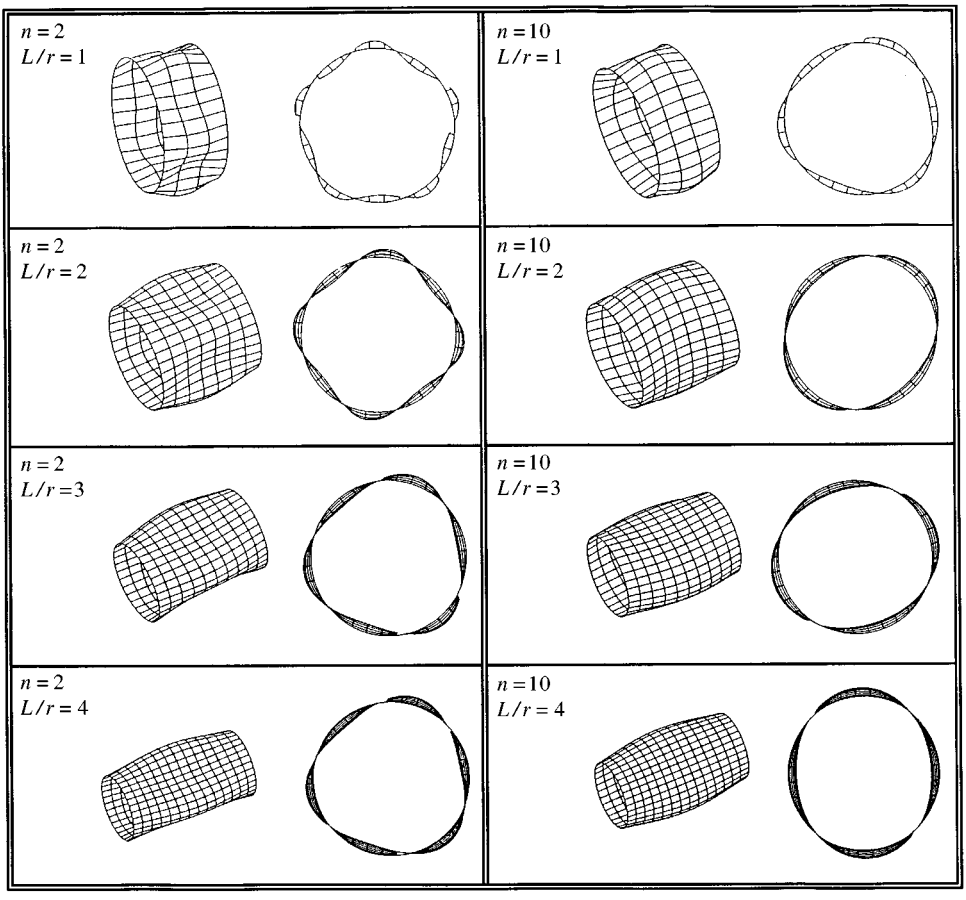

Figure 6. Fundamental vibration mode of $[\pm\theta/90_2/0]_{ns}$ laminated cylindrical shells with two fixed ends and under optimal fiber angles ($r = 10$ cm).

cylindrical shells. From Figure 7(a) we can see that the optimal fiber angle θ of the cylindrical shells decreases with the increase of the cutout size. In addition, under the same d/r ratio, the shell with two simply supported ends has the largest value for the optimal fiber angle. Figure 7(b) shows that under the same d/r ratio, the optimal fundamental frequency is highest for a shell with two fixed ends and lowest for a shell with two simply supported ends. When the d/r ratio is greater than 0·8, the optimal fundamental frequencies of these shells decrease with the increase of the cutout size. However, when the d/r ratio is less than 0·8, the optimal fundamental frequency seems to be insensitive to the cutout size. This phenomenon is quite different from our intuition that introducing a large hole into a shell should cause a reduction in the fundamental natural frequency of the shell. However, previous research did show that introducing a hole into a composite structure does not always reduce the fundamental natural frequency and, in some instances, may increase its fundamental natural frequency [15, 26–28]. This is because the fundamental natural frequency of a composite structure is influenced

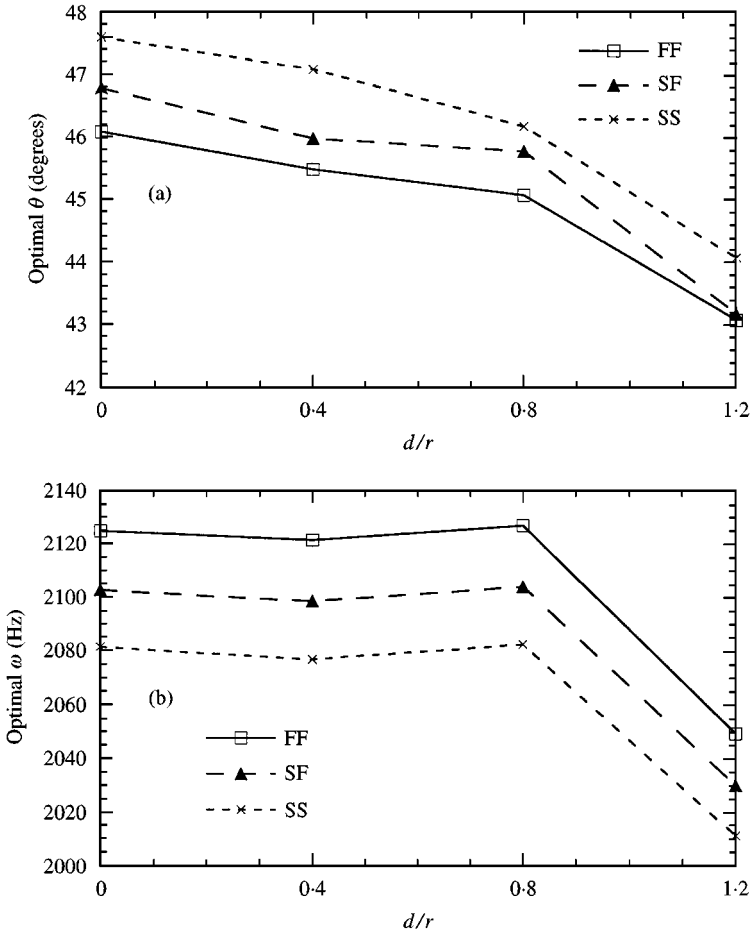

Figure 7. Effects of end conditions and d/r ratio on optimal fiber angle and optimal fundamental frequency of thin ($[\pm\theta/90_2/0]_{2s}$) laminated cylindrical shells with central circular cutouts ($r = 10$ cm, $L = 20$ cm). (a) Optimal fiber angle θ versus d/r ratio; (b) Optimal fundamental frequency ω versus d/r ratio.

not only by a cutout, but also by material orthotropy, end condition, and structural geometry.

Figure 8 shows the optimal fiber angle θ and the associated optimal fundamental frequency ω with respect to the ratio d/r for thick ($[\pm\theta/90_2/0]_{10s}$) laminated cylindrical shells. It can be seen from Figure 8(a) that the optimal fiber angle θ of the thick cylindrical shells varies between 42° and 47° and no longer decreases with increase of the cutout size. Figure 8(b) indicates that the optimal fundamental frequencies of the thick shells decrease with the increase of the cutout size constantly. The reduction in optimal fundamental frequency is more prominent when the cutout size becomes large.

Typical fundamental vibration modes for both thin and thick ($[\pm\theta/90_2/0]_{2s}$ and $[\pm\theta/90_2/0]_{10s}$) cylindrical shells with two fixed ends and under the optimal fiber

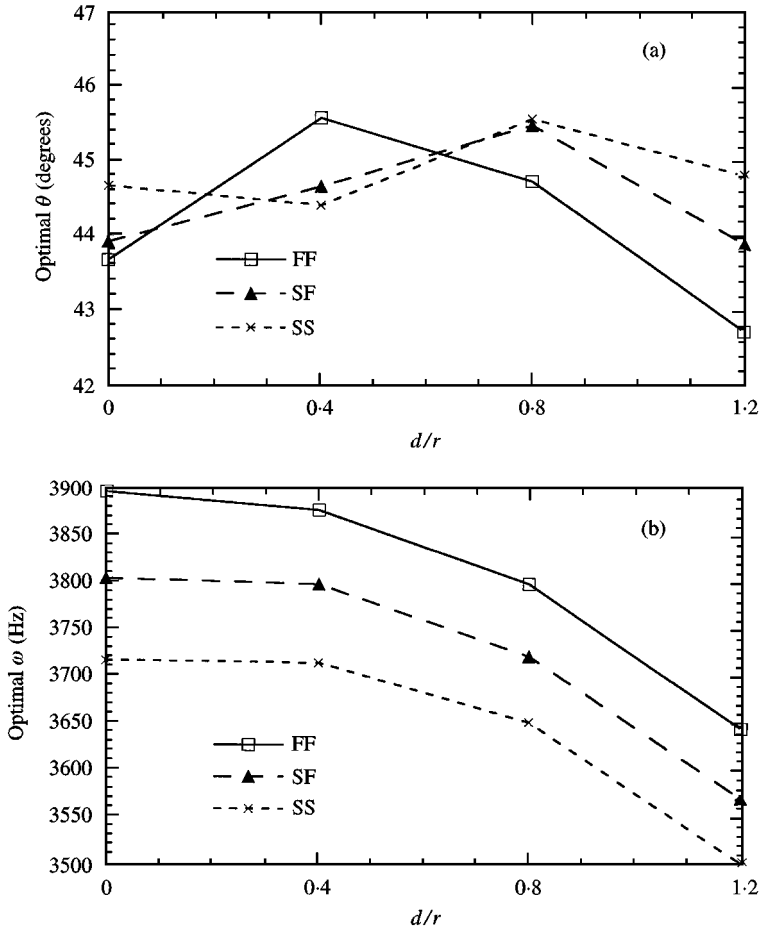

Figure 8. Effects of end conditions and d/r ratio on optimal fiber angle and optimal fundamental frequency of thick ($[\pm\theta/90_2/0]_{10s}$) laminated cylindrical shells with central circular cutouts ($r = 10$ cm, $L = 20$ cm). (a) Optimal fiber angle θ versus d/r ratio; (b) Optimal fundamental frequency ω versus d/r ratio.

orientation are given in Figure 9. These modes show that when the cutout sizes are small, the fundamental vibration modes are global (i.e., vibration of entire shell). However, when the cutout sizes are large, the fundamental vibration modes are local (i.e., vibration of shell area near hole). Similar results are also obtained for laminated cylindrical shells with other end conditions [25].

5.3. LAMINATED CYLINDRICAL SHELLS CONTAINING CENTRAL CIRCULAR CUTOUTS WITH VARIOUS LENGTHS AND END CONDITIONS

In this section, laminated cylindrical shells with $r = 10$ cm are analyzed. The length of the shell, L, varies between 20 cm and 40 cm. These shells contain central circular cutouts with diameter $d = 8$ cm (Figure 3(b)). As before, three types of end

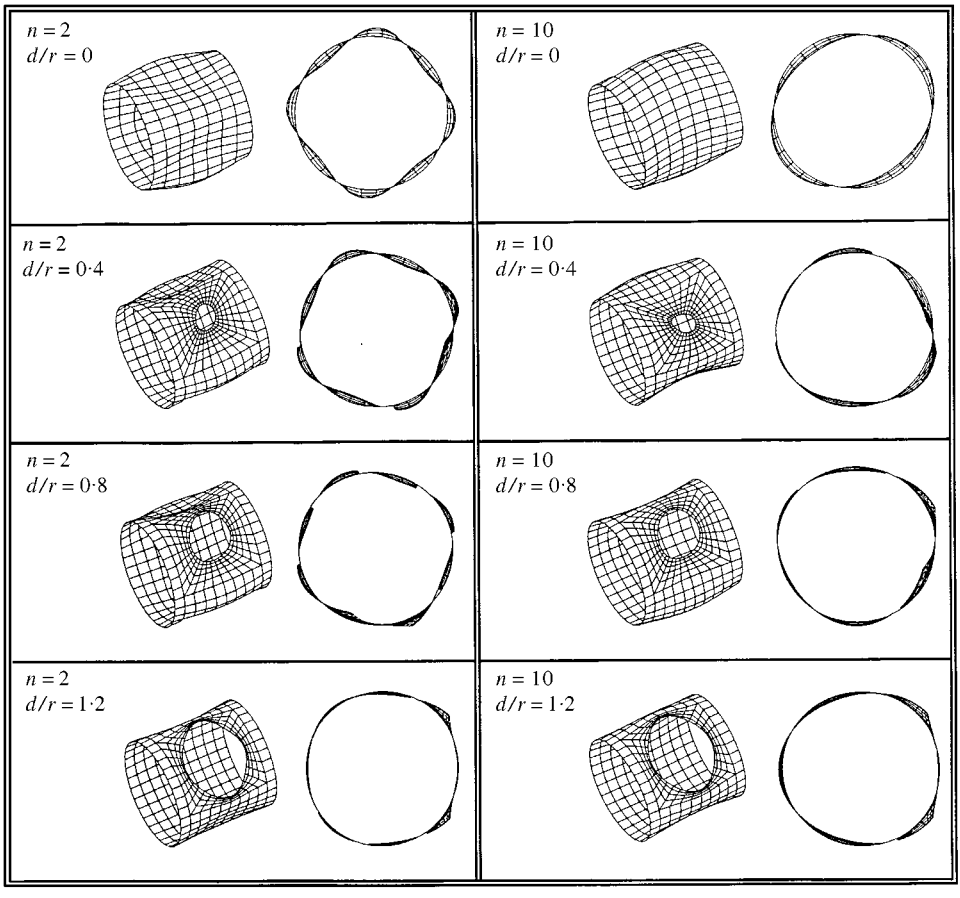

Figure 9. Fundamental vibration mode of $[\pm\theta/90_2/0]_{ns}$ laminated cylindrical shells with central circular cutouts, with two fixed ends and under optimal fiber angles ($r = 10$ cm, $L = 20$ cm).

conditions and two laminate layups, $[\pm\theta/90_2/0]_{2s}$ and $[\pm\theta/90_2/0]_{10s}$, are selected for analysis.

Figures 10 and 11 show the optimal fiber angle θ and the associated optimal fundamental frequency ω with respect to the L/r ratio for thin and thick ($[\pm\theta/90_2/0]_{2s}$ and $[\pm\theta/90_2/0]_{10s}$) laminated cylindrical shells with central circular cutouts. For thin shells, it seems that when L/r ratio is small (say $L/r < 3$), the optimal fiber angles increase with increase of shell length. When L/r ratio is large (say $L/r > 3$), the optimal fiber angles decrease with increase of shell length (Figure 10(a)). For thick shells, when L/r ratio is large (say $L/r > 2{\cdot}5$), the optimal fiber angles seem to approach constant values (Figure 11(a)). Comparing Figure 10(a) and 11(a) with Figures 4(a) and 5(a), we can see that the cutouts have significant effects on the optimal fiber angles of laminated cylindrical shells when the L/r ratio is small (say $L/r < 3$). This effect is more significant for thin shells than that for thick shells. From Figures 10(b) and 11(b) we can see that for both thin and thick shells containing central circular cutouts, their optimal fundamental

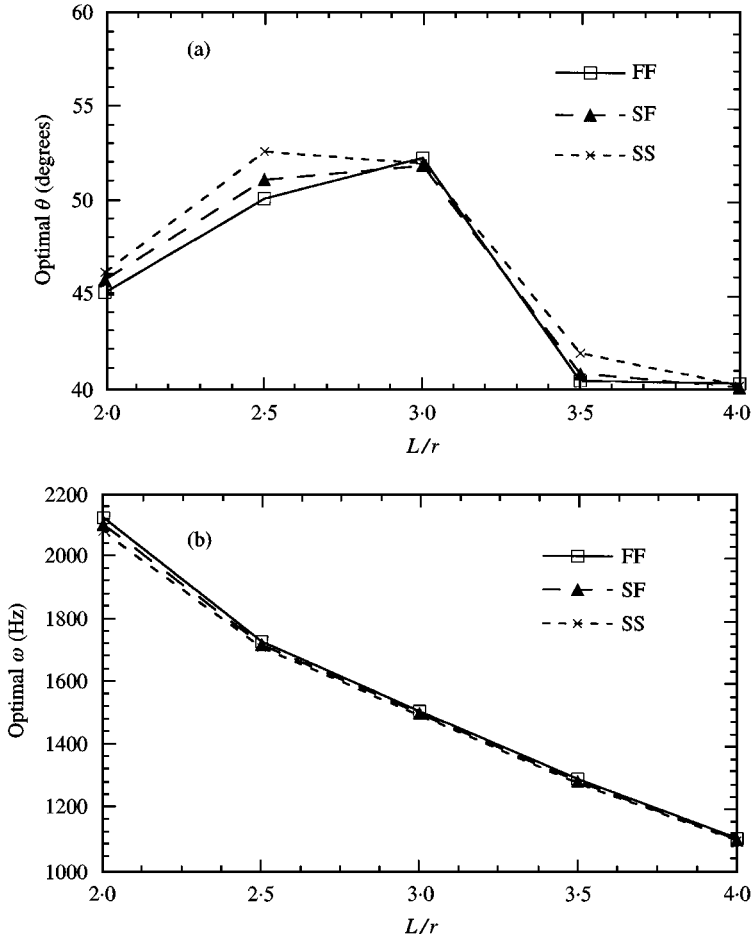

Figure 10. Effects of end conditions and L/r ratio on optimal fiber angle and optimal fundamental frequency of thin ($[\pm\theta/90_2/0]_{2s}$) laminated cylindrical shells with a central circular cutout ($r = 10$ cm, $d = 8$ cm). (a) Optimal fiber angle θ versus L/r ratio; (b) Optimal fundamental frequency ω versus L/r ratio.

frequencies decrease with the increase of L/r ratio. Again, the optimal fundamental frequencies seem to be less sensitive to the end conditions when the L/r ratio becomes large.

Typical fundamental vibration modes for both thin and thick ($[\pm\theta/90_2/0]_{2s}$ and $[\pm\theta/90_2/0]_{10s}$) cylindrical shells containing central circular cutouts with two fixed ends and under optimal fiber orientations are given in Figure 12. Comparing figure 12 with Figure 6, we can observe that when the L/r ratios are small, the cutouts cause the fundamental vibration modes of shells to have significant distortion around the hole area. This distortion is more prominent for a thick shell than for a thin shell. When the L/r ratios are large, the fundamental vibration modes of shells seem to be insensitive to the presence of cutouts. In addition, for thick shells with large L/r ratios, the introduction of cutouts may cause the fundamental

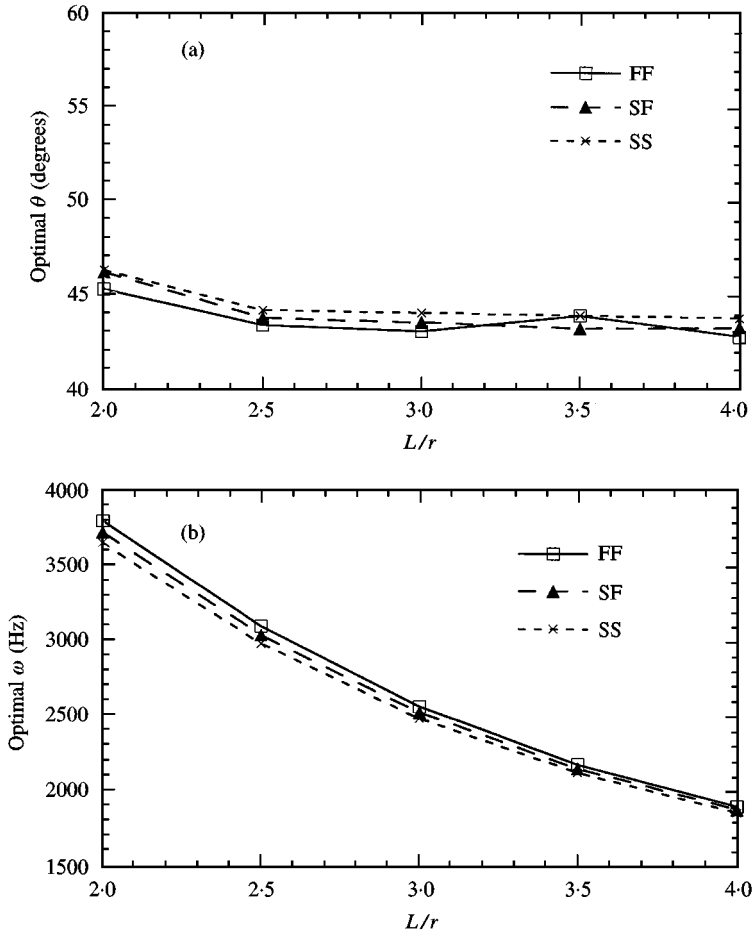

Figure 11. Effects of end conditions and L/r ratio on optimal fiber angle and optimal fundamental frequency of thick ($[\pm\theta/90_2/0]_{10s}$) laminated cylindrical shells with a central circular cutout ($r = 10$ cm, $d = 8$ cm). (a) Optimal fiber angle θ versus L/r ratio; (b) Optimal fundamental frequency ω versus L/r ratio.

vibration modes to have more waves in the circumferential direction. Similar results are also obtained for laminated cylindrical shells with other end conditions [25].

6. CONCLUSIONS

Generally, thickness, end condition, shell length and central circular cutout have significant effects on the optimal fiber angles and optimal fundamental frequencies of $[\pm\theta/90_2/0]_{ns}$ ($n = 2$ and 10) laminated cylindrical shells. To be more specific, the following conclusions may be drawn:

1. Whether laminated cylindrical shells contain cutouts or not, the range of the optimal fiber angle for thick shells is narrower than that for thin shells.

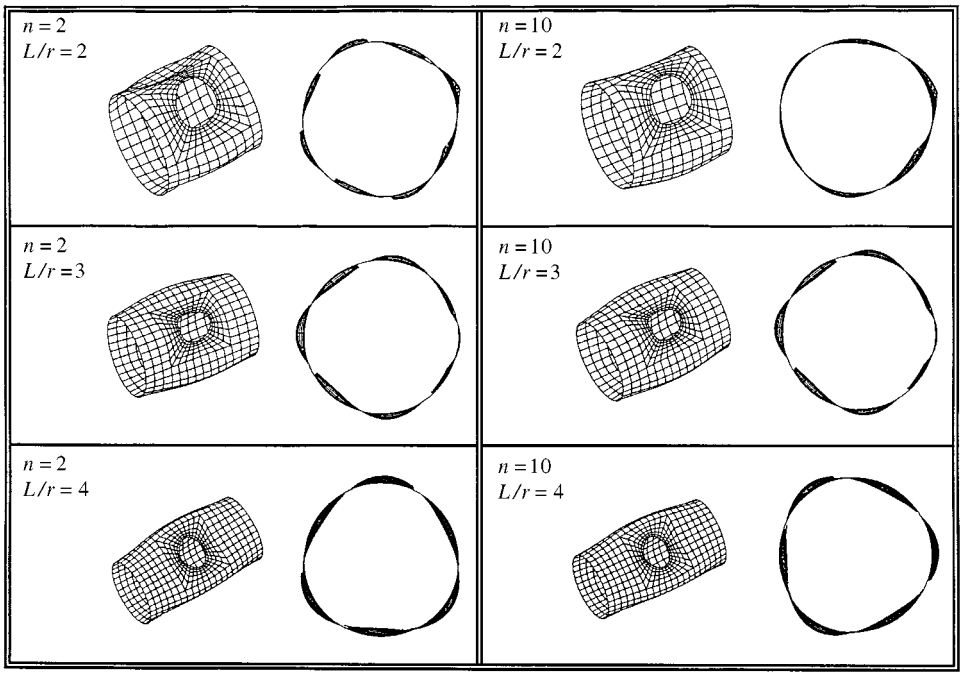

Figure 12. Fundamental vibration mode of $[\pm\theta/90_2/0]_{ns}$ laminated cylindrical shells with central circular cutouts, with two fixed ends and under optimal fiber angles ($r = 10$ cm, $d = 8$ cm).

2. The optimal fundamental frequencies of laminated cylindrical shells decrease with increase of the shell length. Under the same geometry, the optimal fundamental frequency is highest for a shell with two fixed ends and is lowest for a shell with two simply supported ends. However, the optimal fundamental frequencies seem to be less sensitive to the end conditions when the L/r ratio becomes large.
3. The optimal fundamental frequencies of thick laminated cylindrical shells decrease with the increase of the cutout size. The optimal fundamental frequencies of thin laminated cylindrical shells may not decrease with increase of the cutout size.
4. When the shell length or the shell thickness increases, the vibration modes of the cylindrical shells have fewer waves in the circumferential direction.
5. When the cutout sizes are small, the fundamental vibration modes of shells are global. However, when the cutout sizes are large, the fundamental vibration modes of shells are local to the hole.
6. When the L/r ratios are small, the cutouts cause the fundamental vibration modes of shells to have significant distortion around the hole area. This distortion is more prominent for a thick shell than for a thin shell. When the L/r ratios are large, the fundamental vibration modes of shells seem to be insensitive to the presence of cutouts.

REFERENCES

1. A. W. Leissa 1978 *The Shock and Vibration Digest* **10**, 21–35. Recent research in plate vibrations 1973–1976: complicating effects.
2. A. W. Leissa 1981 *The Shock and Vibration Digest* **13**, 19–36. Plate vibrations research 1976–1980: complicating effects.
3. A. W. Leissa 1987 *The Shock and Vibration Digest* **19**, 10–24. Recent studies in plate vibrations: 1981–1985, part II, complicating effects.
4. C. W. Bert, J. L. Baker and D. M. Egle 1969 *Journal of Composite Materials* **3**, 480–499. Free vibrations of multilayer anisotropic cylindrical shells.
5. J. B. Greenberg and Y. Stavsky 1980 *Acta Mechanica* **36**, 15–29. Buckling and vibration of orthotropic composite cylindrical shells.
6. M. E. Vanderpool and C. W. Bert 1981 *AIAA Journal* **19**, 634–641. Vibration of a materially monoclinic thick–wall circular cylindrical shell.
7. I. Sheinman and S. Greif 1984 *Journal of Composite Materials* **18**, 200–215. Dynamic analysis of laminated shells of revolution.
8. N. Alam and N. T. Asnani 1984 *AIAA Journal* **22**, 975–981. Vibration and damping of a multilayered cylindrical shell, part II: numerical results.
9. C. B. Sharma and M. Darvizeh 1987 *Composite Structures* **7**, 123–138. Free vibration of specially orthotropic, multilayered, thin cylindrical shells with various end conditions.
10. N. Alam and N. T. Asnani 1987 *Journal of Composite Materials* **21**, 348–361. Vibration and damping analysis of a fiber reinforced composite material cylindrical shell.
11. R. R. Kumar and Y. V. K. S. Rao 1988 *Computers and Structures* **28**, 717–722. Free vibrations of multilayered thick composite shells.
12. S. Ramakrishna, K. M. Rao and N. S. Rao 1992 *Composite Structures* **21**, 177–185. Free vibration analysis of laminates with circular cutout by hybrid–stress finite element.
13. R. A. Raouf 1994 *Composite Structures* **29**, 259–267. Tailoring the dynamic characteristics of composite panels using fiber orientation.
14. S. Abrate 1994 *Composite Structures* **29**, 269–286. Optimal design of laminated plates and shells.
15. H.-T. Hu and C.-D. Juang 1997 *Journal of Aircraft* **34**, 792–801. Maximization of the fundamental frequencies of laminated curved panels against fiber orientation.
16. C. W. Bert 1991 *The Shock and Vibration Digest* **23**, 9–21. Literature review—research on dynamic behavior of composite and sandwich Plates—V: Part II.
17. L. A. Schmit 1981 *AIAA Journal* **19**, 1249–1263. Structural synthesis—its genesis and development.
18. G. N. Vanderplaats 1984 *Numerical Optimization Techniques for Engineering Design with Applications*, New York: McGraw-Hill, Chapter 2.
19. R. T. Haftka, Z. Gürdal and M. P. Kamat 1990 *Elements of Structural Optimization*, Dordrecht: Kluwer Academic Publishers, Chapter 4, second revised edition.
20. Hibbitt, Karlsson and Sorensen, Inc. 1997 *ABAQUS User, Theory and Verification Manuals*, Version 5.6. Providence, Rhode Island.
21. J. M. Whitney 1973 *Journal of Applied Mechanics* **40**, 302–304. Shear correction factors for orthotropic laminates under static load.
22. E. F. Crawley 1979 *Journal of Composite Materials* **13**, 195–205. The natural modes of graphite/epoxy cantilever plates and shells.
23. R. D. Cook, D. S. Malkus and M. E. Plesha 1989 *Concepts and Applications of Finite Element Analysis*. New York: Wiley, Chapter 13, third edition.
24. K. J. Bathe and E. L. Wilson 1972 *Journal of Engineering Mechanics Division, ASCE* **98**, 1471–1485. Large eigenvalue problems in dynamic analysis.
25. J.-Y. Tsai 1996 *M.S. Thesis, Department of Civil Engineering, National Cheng Kung University, Tainan, Taiwan, R.O.C.* Influence of geometry and end conditions on optimal fundamental frequencies and associated optimal fiber angles of symmetrically laminated cylindrical shells.

26. H. P. Lee, S. P. Lim and S. T. Chow 1987 *Composite Structures* **8**, 63–81. Free vibration of composite rectangular plates with rectangular cutouts.
27. S. Ramakrishna, K. M. Rao and N. S. Rao 1992 *Composite Structures* **21**, 177–185. Free vibration analysis of laminates with circular cutout by hybrid-stress finite element.
28. H.-T. Hu and M.-H. Ho 1996 *Journal of Reinforced Plastics and Composites* **15**, 877–893. Influence of geometry and end conditions on optimal fundamental natural frequencies of symmetrically laminated plates.